Damping of Crystallization Waves at the Solid-Liquid Interface of Helium

C. L. Wang and G. Agnolet
Department of Physics, Texas A&M University, College Station, Texas 77843
(Received 16 September 1991; revised manuscript received 13 April 1992)

The low-temperature behavior of ^{4}He crystallization waves has been studied from 0.03 to 0.5 K. From the damping of these waves we have determined the interfacial growth resistance, $(Km)^{-1}$. At the lowest temperatures, $(Km)^{-1}$ is consistent with the assumption that the growth velocity is limited by the scattering of ballistic phonons by the moving interface. Above $T \approx 0.25$ K, $(Km)^{-1}$ increases more slowly with temperature, indicating a decrease in the phonon contribution from that observed at lower temperatures.

PACS numbers: 67.80.Cx, 61.50.Cj, 68.45.Kg, 68.45.Nj

The ^{4}He solid-liquid interface, although quantum in nature, has proved to be an ideal system for studying interfacial phenomena found in more classical systems [1]. Many of the material properties of helium make it possible to *directly* observe interfacial details that are often hidden in more conventional materials, thereby enabling one to study the intrinsic physical mechanisms of crystal growth and equilibrium. The rapid equilibration rates in this system often make it possible to use techniques typically used in studies of the liquid-vapor interface [2].

Three crystallographic surfaces of ^{4}He hcp crystals are known to exhibit roughening transitions [3]. Below the roughening transition temperature, these surfaces develop atomically smooth facets with very few defects. Other surface orientations remain atomically rough even to very low temperatures [4]. Because of the superfluid nature of the liquid and the small latent heat, these rough surfaces can exhibit extremely rapid growth dynamics. In fact, the interface can support wavelike motions that are analogous to the capillary or gravity waves found at liquid surfaces. These deformations of the interface move across the interface by alternately *growing* and *melting* the solid in the direction of motion. As such, these "crystallization" waves can be used as a direct and sensitive probe of the interfacial growth dynamics.

Crystallization waves were first predicted by Andreev and Parshin [5] (AP) based on ideas of quantum delocalization of surface defects. They conjectured that at sufficiently low temperatures the growth velocity would be limited by the scattering of bulk thermal excitations by the moving interface. In particular, at the lowest temperatures, the growth resistance $(Km)^{-1} = \Delta\mu/v_i$ (v_i is the interfacial velocity and $\Delta\mu$ is the chemical potential difference across the interface) would increase as T^4 due to phonons and, at higher temperatures, would increase exponentially corresponding to the temperature dependence of the roton density. Other calculations [6–9] have verified these ideas and have made specific predictions as to the range of validity and magnitude of these effects.

Keshishev, Parshin, and Babkin [10] (KPB) were the first to observe these waves and verify their dispersion $\omega(k)$. From measurements of the attenuation of the waves, they showed that the temperature dependence of $(Km)^{-1}$ agreed reasonably well with the predictions of AP. An interesting but unexplained feature of their data was that $(Km)^{-1}$ did not extrapolate to zero at $T = 0$. In addition, these zero-temperature offsets varied with the measuring frequency and crystal orientation.

We have extended the measurements of KPB to lower temperatures so that a more exacting test of existing theoretical predictions can be made. In our experiment, we excite standing crystallization waves within the confining boundaries of our experimental cell. To maintain a horizontal interface across the crystal, two walls of the cell are tilted to provide the correct contact angle [11] between the interface and the wall ($\theta_{cw} \approx 137°$). (A cross-sectional view is shown in Fig. 1.) Waves are generated by applying an oscillating voltage to an interdigital capacitor mounted on one wall of the cell. The detector consists of a second interdigital capacitor mounted on the opposite wall that, together with a fixed inductor,

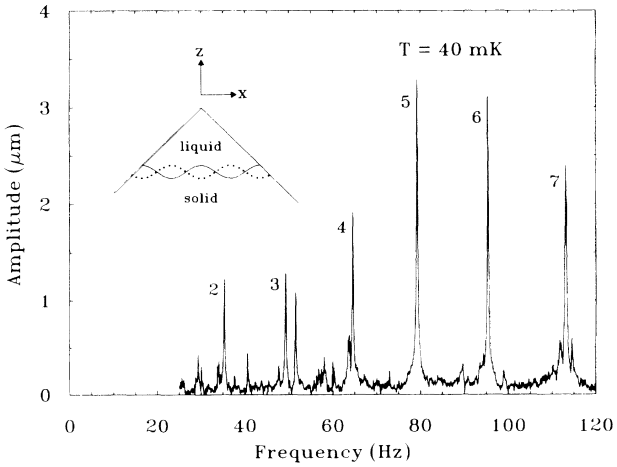

FIG. 1. Resonances corresponding to standing crystallization waves. Inset: A schematic cross section of the experimental geometry. The fundamental mode ($\approx$ 22 Hz) is not shown as it was obscured by extraneous noise.

forms the resonator of a tunnel diode circuit. Capacitance variations in the detector produced by interfacial motion are converted to a voltage by demodulating the resonant frequency of the tunnel diode circuit.

Helium crystals are grown from ultrapure helium gas [12] (4.54 ppb ^{3}He) at constant temperature ($T \sim 1$ K). The interface is cycled at this temperature by repeated melting and growing before cooling to the measuring temperature. Typical growth rates are 2 μm s^{-1}.

The orientation of the crystal surface can be controlled to some extent by nucleating the helium crystal on the surface of a clean graphite crystal [13] mounted on a platform at the bottom of the cell. By rotating the platform *in situ* with an electromagnetically activated ratchet before nucleating a new crystal, the angle θ between the surface normal and crystalline c axis [0001] of the nucleated crystal can be varied over a range of 90° without warming the cryostat. The orientation is checked by measuring the sound velocity in the crystal with ultrasound transducers. We present data from two orientations ($\theta = 33° \pm 5°$ and $5° \pm 5°$). No information is available on the orientation with respect to the [10$\bar{1}$0] axis.

The normal modes of the interface can be easily identified by monitoring the response of the interface while sweeping the frequency of the drive voltage. Figure 1 illustrates some of the low-frequency resonant modes for a rectangular interface with dimensions 0.95 and 2 cm along the x and y axes, respectively.

The structure of these modes is determined by the potential flow of the liquid above the interface and by the gravitational and interfacial free energies associated with distortions of the interface. Because of the complexities introduced by the tilted walls of the cell, it is necessary to solve for the normal modes numerically. One can expand the liquid flow potential $\phi(x,z)$ ($v_\ell = \nabla\phi$ where v_ℓ is the liquid velocity) in terms of solutions to Laplace's equation that satisfy the Neumann boundary conditions at the fixed walls. Here we have assumed that the motion of the interface is independent of the y coordinate. To determine the expansion coefficients, we require the solution to satisfy the interfacial wave equation of the free boundary at the interface ($z = -h$) [10, 14],

$$-\omega^2\phi(x,-h) = \left[g\frac{\rho_\ell}{\rho_c - \rho_\ell} - \tilde{\alpha}\frac{\rho_\ell}{(\rho_c-\rho_\ell)^2}\frac{\partial^2}{\partial x^2}\right]\left.\frac{\partial\phi}{\partial z}\right|_{z=-h}, \quad (1)$$

where h is the vertical position of the interface measured from the apex of the cell, g is the acceleration of gravity, ρ_c and ρ_ℓ are the densities of the crystal and liquid, respectively, and ω is the frequency. Here $\tilde{\alpha} = \alpha + \partial^2\alpha/\partial n_x^2$ denotes the surface stiffness where α is the surface free energy and n_x is the component of the surface normal in the x direction. We also require that the wave profile $\zeta(x)$, defined by

$$\frac{\partial\zeta}{\partial t} = -\frac{\rho_\ell}{\rho_c - \rho_\ell}\left.\frac{\partial\phi}{\partial z}\right|_{z=-h}, \quad (2)$$

obeys open boundary conditions corresponding to fixing the contact angle at the interface-wall boundary.

A typical set of resonant frequencies is shown in Fig. 2. In the limit of high frequencies or short wavelengths, the surface stiffness dominates the energetics. Furthermore, the liquid flow field is highly localized near the moving interface and is therefore relatively independent of the far boundary conditions. In this limit, the frequency should approach the standard result for capillary waves,

$$\omega^2 = \tilde{\alpha}\frac{\rho_\ell}{(\rho_c-\rho_\ell)^2}\left(\frac{2\pi}{\lambda}\right)^3 = \tilde{\alpha}\frac{\rho_\ell}{(\rho_c-\rho_\ell)^2}\left(\frac{\pi}{L}\right)^3 n^3, \quad (3)$$

where λ is the wavelength and $L = 2h\tan(\theta_{cw} - 90°)$ is the length of the interface. At high frequencies, the data asymptotically approach a 3/2 power law indicated by the line in Fig. 2. The departure from this power law at lower frequencies indicates the crossover to the gravity-dominated region ($\omega \sim \lambda^{-1/2}$).

Using the normal-mode calculations, we can fit the entire set of resonant frequencies with only two parameters, $\tilde{\alpha}$ and h. The percentage deviations between the experimental and fitted resonant frequencies are shown in Fig. 2. Although the resulting values for h are consistent with independent measurements of h, the fitted values of $\tilde{\alpha}$ (0.045–0.065 erg cm^{-2}) are smaller than previously reported values [1, 15] (0.08–0.36 erg cm^{-2}). We do not understand this discrepancy, but as we shall see, the value of $\tilde{\alpha}$ only weakly affects the determination of the growth resistance.

The damping coefficient $\gamma = -(\partial E/\partial t)/2E$ is obtained by fitting the resonance curve of a mode with

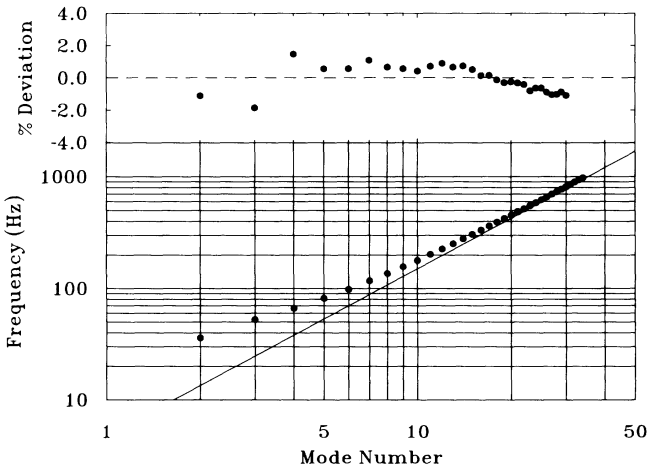

FIG. 2. The measured normal-mode frequencies plotted against mode number. The line indicates the 3/2-power-law dependence expected for capillary waves. Also shown are the deviations determined from the fit of the experimental resonant frequencies using the normal-mode calculations.

a Lorentzian line shape. By equating the rate of energy loss to the rate of entropy production $-(\partial E/\partial t) = T(\partial S/\partial t) = \rho_c v_i \Delta\mu$ one can relate the growth resistance to γ [6, 14]:

$$(Km)^{-1} = -\gamma \frac{2(\rho_c - \rho_\ell)^2 \int dxdy\, \phi(\partial\phi/\partial z)|_{z=-h}}{\rho_c \rho_\ell \int dxdy (\partial\phi/\partial z)^2|_{z=-h}}, \quad (4)$$

where each integral is evaluated over the area of the interface using the functional form of the normal modes. The proportionality constant between γ and $(Km)^{-1}$ depends primarily on the shape of the wave profile and the geometry of the interface and, at high frequencies, is proportional to the wave vector $k = n\pi/L$ because of the localized character of these modes. Since the wave profiles only weakly depend on $\tilde{\alpha}$, values obtained for $(Km)^{-1}$ should not be sensitive to the fitted values of $\tilde{\alpha}$.

Figure 3 shows the temperature dependence of the effective growth resistance for two crystal orientations. In the limit that the mean free path of the thermal excitations is large compared to the wavelength of the crystallization waves (ballistic regime), $(Km)^{-1}$ should be independent of the mode or wave vector. If other dissipation mechanisms, such as the bulk viscosity, were to contribute to γ, then $(Km)^{-1}$ as determined by the above equation would, in general, be mode dependent. The close agreement between values of $(Km)^{-1}$ determined from different modes ($n = 2$, 5, and 10) strongly suggests that we can neglect such dissipation processes. Within the accuracy of the measurements, we also find no significant difference in $(Km)^{-1}$ for the two orientations.

At low temperatures $(Km)^{-1}$ does not extrapolate to zero but instead approaches a constant value (typically 0.002–0.004 cm s^{-1}). As suggested by KPB, this excess dissipation may be due to dislocations or defects within the crystal. In our experiments, another source of dissipation could be the pinning of the interface at wall-interface boundaries. We looked for such an edge effect by changing the size of the interface and thereby the relative weights of bulk and edge contributions but found no significant correlations with the value of the excess dissipation.

The solid line in Fig. 3 represents the theoretical phonon contribution [7]. To assist in making the comparison, the excess resistance has been added to the phonon contribution [$(Km)^{-1}_{\text{phonon}} = 3.19T^4$ cm s^{-1} K^{-4}] [16]. Above $T \approx 0.25$ K, $(Km)^{-1}$ increases more slowly with temperature and consequently falls significantly below the predicted phonon contribution. We attribute the rapid increase of $(Km)^{-1}$ above 0.4 K to the exponential increase expected for the roton contribution.

To analyze the temperature dependence of the growth resistance, we first note that roton contributions should be insignificant below 0.35 K. Consequently, by plotting the data below 0.4 K as a function of T^4, we can emphasize the phonon contributions (Fig. 4). For clarity, only one data set is shown; other data sets show similar behavior. Below 0.25 K, the data are consistent with a T^4 dependence with a prefactor of 2.79 cm s^{-1} K^{-4}, in good agreement with the theoretical estimates [7] (3.06–3.32 cm s^{-1} K^{-4}). (Values obtained from the other data sets range from 2.7 to 3.5 cm s^{-1} K^{-4}.)

We conjecture that the dramatic change in the temperature dependence at 0.25 K is caused by a crossover of the crystal phonons from ballistic to hydrodynamic

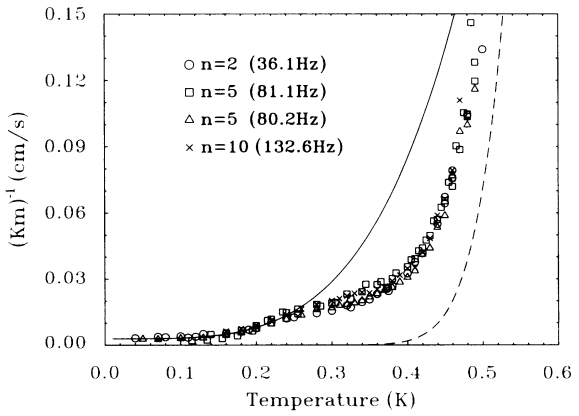

FIG. 3. The growth resistance determined from different normal modes n. Data from two crystal orientations are shown (○ and □, $\theta \approx 33°$ and △ and ×, $\theta \approx 5°$). The solid and dashed curves represent the contributions associated with the scattering of phonons and rotons, respectively.

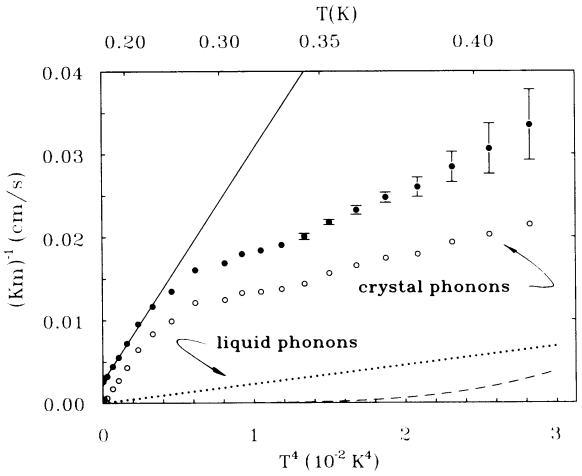

FIG. 4. $(Km)^{-1}$ (•) plotted vs T^4 to emphasize the phonon contribution. The solid line indicates the fit by the low-temperature phonon contribution [$2.79T^4$ cm s^{-1} K^{-4}] and the $T = 0$ offset [0.0026 cm s^{-1}]. The crystal phonon contribution (○) is computed by subtracting the estimated contributions of the liquid phonons (dotted line) and rotons (dashed line) and the $T = 0$ offset. Error bars are derived from fits of the resonance curves of the mode with a Lorentzian line shape.

behavior. From estimates [17] of the phonon mean free path in the crystal such a crossover would be expected above 0.2 K. The degree to which the phonon gas is hydrodynamic can be characterized by the average velocity of the crystal phonons relative to the crystal lattice, v_{nc}. (In the ballistic and hydrodynamic limits v_{nc} equals 0 and v_i, respectively.) Within this approximation [7] the dissipation due to the crystal phonons is reduced by a factor of f_c^2 where $f_c = 1 - v_{nc}/v_i$. Our data indicate that f_c decreases from its value of 1 at 0.22 K to a value of 0.59 at 0.4 K, suggesting that even at 0.4 K some of the crystal phonons remain ballistic.

Because of the limited temperature range of the data and the difficulty in reliably extrapolating the phonon contribution to higher temperatures, we can only show the overall consistency of our data with the theoretical predictions for the roton contribution. By assuming the remnant phonon contribution continues to scale above 0.4 K as T^4, we can fit the additional contribution with $(Km)^{-1}_{\text{roton}} = (2\pi p_0^4/h^3\rho_c)(1-\xi)\exp(-\Delta/T)$ cm s^{-1} where the roton parameters p_0 and Δ are chosen to have their equilibrium values on the melting curve [7, 9]. The factor $1 - \xi$ represents a correction for the anomalous "Andreev" scattering of the rotons from the interface. Values for $1 - \xi$ range from 0.5 to 0.6 in agreement with previously measured values (see Ref. [9]). The roton contribution is shown as dashed lines in Figs. 3 and 4.

Comparing our values for $(Km)^{-1}$ with those of KPB, we find that both show similar temperature dependences above 0.36 K except that the data of KPB have larger zero-temperature offsets. We believe that the apparent agreement of their data with the theoretical phonon contribution is due to the influence of the non-negligible roton contributions at these higher temperatures. In going to much lower temperatures, we have established that the ballistic regime only extends to 0.25 K.

The authors would like to thank D.O. Edwards, W.M. Saslow, M.V. Jarić, and P. Crowell for stimulating discussions and suggestions. One of us (G.A.) would like to thank AT&T Bell Laboratories where this experiment was initiated. This work was supported by the NSF, Division of Materials Research (DMR-8451893) and by the State of Texas, Advanced Research Program (3046 and 10266-145).

[1] S. Balibar and B. Castaing, Surf. Sci. Rep. **5**, 87 (1985); S.G. Lipson and E. Polturak, Prog. Low Temp. Phys. **11**, 127 (1987).

[2] S. Balibar, D.O. Edwards, and C. Laroche, Phys. Rev. Lett. **42**, 782 (1979).

[3] S. Balibar and B. Castaing, J. Phys. Lett. **41**, 1329 (1980); J. Avron, L. Balfour, C. Kuper, S. Lipson, and L. Shulman, Phys. Rev. Lett. **45**, 814 (1980); K.O. Keshishev, A. Ya Parshin, and A.V. Babkin, Zh. Eksp. Teor. Fiz. **80**, 716 (1981) [Sov. Phys. JETP **53**, 362 (1981)].

[4] G. Agnolet, D.D. Osheroff, and W.O. Sprenger, Jpn. J. Appl. Phys. **26**, Suppl. 26-3, 355 (1987).

[5] A.F. Andreev and A. Ya Parshin, Zh. Eksp. Teor. Fiz. **75**, 1511 (1978) [Sov. Phys. JETP **48**, 763 (1978)].

[6] A.F. Andreev and V.G. Knizhnik, Zh. Eksp. Teor. Fiz. **83**, 416 (1982) [Sov. Phys. JETP **56**, 226 (1982)].

[7] R.M. Bowley and D.O. Edwards, J. Phys. (Paris), **44**, 723 (1983).

[8] P. Nozières and M. Uwaha, J. Phys. (Paris), **48**, 329 (1987).

[9] D.O. Edwards, S. Mukherjee, and M.S. Petterson, Phys. Rev. Lett. **64**, 904 (1990).

[10] K.O. Keshishev, A. Ya Parshin, and A.V. Babkin, Pis'ma Zh. Eksp. Teor. Fiz. **30**, 63 (1979) [JETP Lett. **30**, 56 (1979)]; a review of this work is given by A. Ya Parshin, in *Low Temperature Physics*, edited by A.S. Borovik-Romanov (MIR Publishers, Moscow, U.S.S.R., 1985), p. 15.

[11] J. Landau, S.G. Lipson, L.M. Määttänen, L.S. Balfour, and D.O. Edwards, Phys. Rev. Lett. **45**, 31 (1980).

[12] Bureau of Mines, Amarillo, Texas 79101.

[13] S. Balibar, B. Castaing, and C. Laroche, J. Phys. (Paris), Lett. **41**, L283 (1980).

[14] A.F. Andreev, Prog. Low Temp. Phys. **8**, 67 (1982).

[15] O.A. Andreeva and K.O. Keshishev, Pis'ma Zh. Eksp. Teor. Fiz. **52**, 799 (1990) [JETP Lett. **52**, 164 (1990)].

[16] Only an average value is plotted since $(Km)^{-1}_{\text{phonon}}$ is expected to depend weakly on orientation (3.32 to $3.06T^4$ cm s^{-1} K^{-4}).

[17] A.A. Golub and S.V. Svatko, Sov. Fiz. Nizk. Temp. **6**, 957 (1980); **7**, 413 (1981) [Sov. J. Low Temp. Phys. **6**, 465 (1980); **7**, 203 (1981)].